

## Sea-level change during MIS 5a based on submerged speleothems from the eastern Adriatic Sea (Croatia)

Maša Surić<sup>a,\*</sup>, David A. Richards<sup>b</sup>, Dirk L. Hoffmann<sup>b</sup>, Darko Tibiljaš<sup>c</sup>, Mladen Juračić<sup>d</sup>

<sup>a</sup> Department of Geography, University of Zadar, Tudmanova 24 i, 23000 Zadar, Croatia

<sup>b</sup> Bristol Isotope Group, School of Geographical Sciences, University of Bristol, University Road, Bristol BS8 1SS, UK

<sup>c</sup> Department of Geology, Faculty of Science, University of Zagreb, Horvatovac bb, 10000 Zagreb, Croatia

<sup>d</sup> Department of Geology, Faculty of Science, University of Zagreb, Horvatovac 102 a, 10000 Zagreb, Croatia

### ARTICLE INFO

#### Article history:

Received 23 May 2008

Received in revised form 7 January 2009

Accepted 8 March 2009

#### Keywords:

sea-level change

MIS 5a

submerged speleothems

U–Th dating

Adriatic Sea

### ABSTRACT

Two stalagmites were collected from below sea level in U Vode Pit on the Krk Island, eastern Adriatic Sea, at elevations of –14.5 and –18.8 m. They exhibit a growth history indicating a double high sea-level stand during marine isotope stage (MIS) 5a (~87–77 ka). Thin layers of halite and gypsum were found to be associated with hiatuses in speleothem growth probably caused by seawater inundation during sea-level highstands. These mineral deposits are likely to have been precipitated during marine regression phases under evaporitic conditions. We constrain the age of the speleothem growth below and above growth hiatuses, and hence timing of possible marine incursions, using multi-collector inductively coupled plasma mass-spectrometry (MC-ICPMS) U–Th techniques. Age estimates indicate that, during MIS 5a, relative sea-level elevations were greater than –14.5 m from ~87 to ~82 ka and –18.8 m from ~77 to ~64 ka, and constrained to be lower than –18.8 m from >93 to ~90 ka, ~82 to ~77 ka and ~64 to ~54 ka, assuming no tectonic adjustment. However, present speleothem depths could indicate long term regional tectonics.

© 2009 Elsevier B.V. All rights reserved.

### 1. Introduction

Eustatic sea level during the last interglacial–glacial period has been derived principally from radiometric ages and elevations of fossil shoreline deposits such as corals and shells, adjusted for tectonic and glacio-hydro-isostatic components (Chappell and Shackleton, 1986; Hearty et al., 1986; Muhs et al., 1994; Murray-Wallace, 2002; Cutler et al., 2003; Wehmiller et al., 2004), or model-based results from oxygen-isotope data in ocean sediments (Lea et al., 2002; Waelbroeck et al., 2002; Siddall et al., 2003). To provide valuable constraints on both the eustatic component of sea-level change and the spatially variable glacio-hydro-isostatic response of the earth and ocean to the growth and decay of ice sheets, we need sea-level estimates from a host of disparate locations in differing tectonic regimes (e.g. Lambeck, 1995; Pirazzoli, 1996; Lambeck and Bard, 2000). In particular, it is critical that more direct sea-level evidence is obtained for periods when sea levels were lower than present during the interglacial–glacial cycle. Sea levels are less well constrained for these times because shoreline evidence is emergent only in areas that have been subject to substantial tectonic or isostatic uplift. Here, we take advantage of submerged cave deposits that record hiatuses in growth

after drowning by rising sea levels to provide additional constraints on the timing and elevation of past sea-level highs. We derive data here for the eastern Adriatic coast, which has yielded a reasonable amount of evidence for the tectonic history of the late Holocene period in the form of archaeological markers and tidal notches (e.g. Faivre and Fouache, 2003; Benac et al., 2004; Antonioli et al., 2007; Benac et al., 2008) but little is known for longer timescales.

In order to reconstruct relative sea-level changes on the eastern Adriatic coast, speleothems (stalagmites, stalactites and flowstones) were collected from submerged caves and pits along the Croatian coast. Their growth provides an unambiguous indicator of former low sea levels and can be used to constrain past sea-level elevation and timing. Similar research, for example, has been undertaken on submerged speleothems from the Tyrrhenian Sea (Bard et al., 2002; Antonioli et al., 2004), from the Ionian Sea (Dutton et al., 2009), Bahamas archipelago (Richards et al., 1994; Lundberg and Ford, 1994), Balearic islands (Fornós et al., 2002; Onac et al., 2006) and from eastern Adriatic Sea (Vrhovec et al., 2001; Surić et al., 2005). For submerged samples, the youngest calcite deposition provides a *maximum* age constraint for the timing of the marine transgression that caused a cessation of growth, while earliest growth provides a *minimum* age constraint on the initiation of growth after sea level regression. We stress the words maximum and minimum because other factors such as shifts in flow routing or changes in water chemistry, flooding, aridity etc. can also cause a cessation in calcite deposition (Richards and Dorale, 2003). For growth discontinuities that occurred prior to the final

\* Corresponding author. Tel.: +385 23 345022; fax: +385 23 311282.

E-mail addresses: [msuric@unizd.hr](mailto:msuric@unizd.hr) (M. Surić), [david.richards@bristol.ac.uk](mailto:david.richards@bristol.ac.uk) (D.A. Richards), [dirk.hoffmann@bristol.ac.uk](mailto:dirk.hoffmann@bristol.ac.uk) (D.L. Hoffmann), [dtibiljas@public.srce.hr](mailto:dtibiljas@public.srce.hr) (D. Tibiljaš), [mjuracic@geol.pmf.hr](mailto:mjuracic@geol.pmf.hr) (M. Juračić).

cessation, one can use definitive evidence for marine incursion such as biogenic crust overgrowths, as exhibited on material from the Tyrrhenian coast (Bard et al., 2002; Antonioli et al., 2004), or mineral assemblages typical of marine phreatic conditions, to provide robust elevation and timing constraints.

Two stalagmites, from  $-14.5$  and  $-18.8$  m in U Vode Pit on the Krk Island, appear to record a marine transgression marked with growth hiatuses and minerals associated with marine evaporitic conditions. In discussing sea-level elevations in this text, we quote all values with respect to present mean sea level, where a negative value is an indication of depth below the present mean sea level.

## 2. Geological setting and samples

The Adriatic Sea is a semi-enclosed epicontinental basin, situated between the Apennines and Dinaric mountain ranges, characterized by a relatively shallow northern section (0 to  $-120$  m) with a low gradient ( $0.02^\circ$ ). The bathymetry is such that past spatial extent was sensitive to eustatic sea-level changes. After the last glacial maximum (LGM), for example, postglacial sea-level rise generated an eight-fold widening of the shelf area (Correggiari et al., 1996; Cattaneo et al., 2003). Much of the coastal (submarine and subaerial) eastern Adriatic and Croatia is karstic, developed mostly in Cretaceous and Palaeogene limestones. After typical carbonate platform sedimentation throughout Mesozoic and Early Palaeogene, collision of the Adria (Apulia) plate and Hercynian European continent during the Alpine orogeny caused a disintegration of the Adriatic platform, and thick carbonate deposits ( $>8$  km, Velić, 2007) intensively folded, faulted and overthrust, were then exposed to exogenic processes resulting in its karstification (Vlahović et al., 2002, 2005). After the first phase of structural displacement (collision),

deformation continued as a shallow subduction in a NE direction forming a thin-skinned thrust system (Blašković, 1999; Picha, 2002). It resulted in a predominance of horizontal displacement in a broader zone, with some narrow localities with pronounced vertical movements. According to Quaternary rockfall breccia, intensive tectonic activity occurred in the post-Pliocene period (Blašković, 1999). Recent GPS measurements also reveal a complex tectonic activity of this area (Altiner et al., 2006).

During global sea-level lowstands, including that associated with the LGM much of the coastal submarine karst (caves, pits with speleothem deposits) would have been above sea level and affected by karstification processes. These karst landforms were then periodically submerged during sea-level highstands. So far, more than 230 submarine caves and pits have been discovered along the Croatian coast and most of them have been explored. More than 140 caves contain speleothems (Surić, 2006) and, currently, the deepest speleothems found within them are those from the submarine in front of Brač Island from  $-71$  m (Garašić, 2006).

Krk Island is the second largest Croatian island and situated in the northern part of the Adriatic Sea (Fig. 1). Two stalagmites, K-14 and K-18, were collected from  $-14.5$  m and  $-18.8$  m, respectively, in U Vode Pit, situated in the southern part of the island. This karstic void is a vertical shaft formed in Upper Cretaceous limestone and is well decorated with speleothems. It is not a completely submarine feature – the entrance of the pit is above present sea level at an elevation of  $5.5$  m. The floor of U Vode Pit has an elevation of  $-24$  m. There is free circulation between the cave and the open sea, and marine organisms (serpulids) are observed within the void. There is a thin brackish water lens of  $0.5$  m.

The uppermost parts of stalagmites K-14 and K-18 (26 and 15 cm, respectively) were sampled from their growth position. Surfaces of

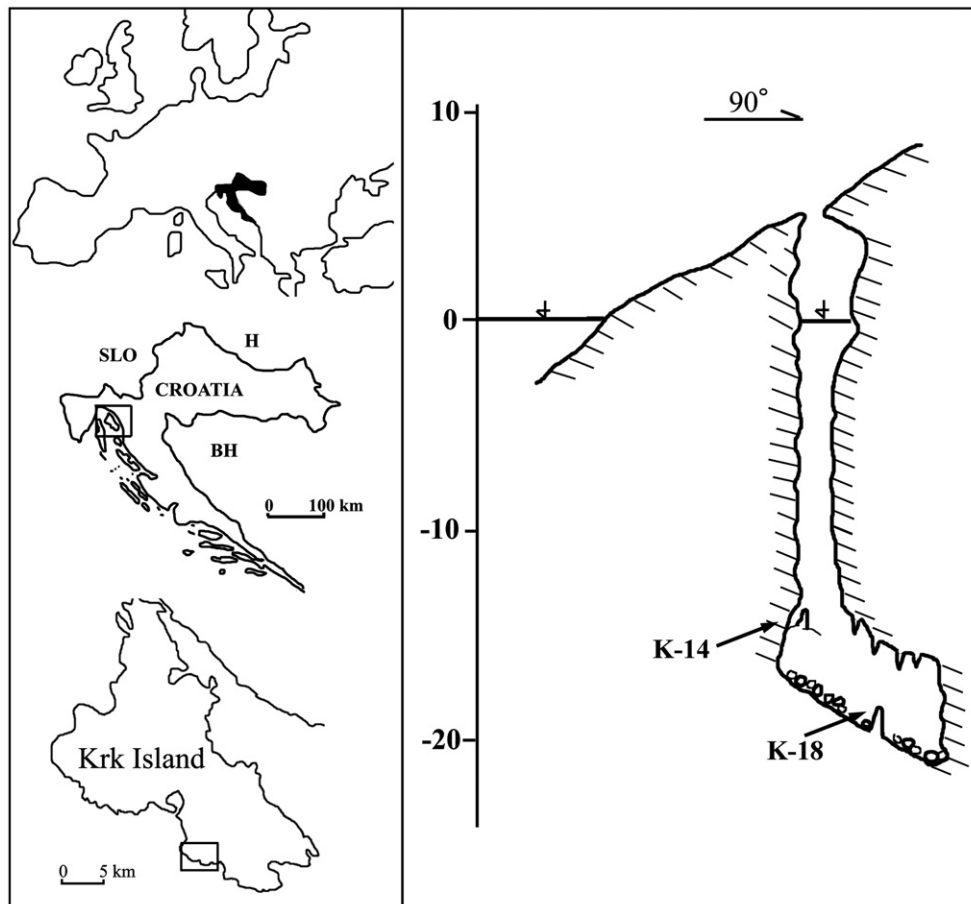


Fig. 1. Location map and cross-section of U Vode Pit, Krk, Croatia showing the locations of the sampled speleothems.

stalagmites K-14 and K-18 are partly covered with marine biogenic overgrowth that consists of exclusively faunal species with dominance of Polychaeta (serpulids), belonging to biocenosis of caves and ducts in complete darkness. This indicates that a stable marine environment has been maintained in the recent past below – 14 m. Each stalagmite was sectioned along the growth axis and polished to reveal the internal growth stratigraphy. Both speleothems are relatively similar in terms of colour, morphology and crystallography of speleothem carbonate (Fig. 2). Calcite material ranges from porous and opaque to dense, translucent (darker sections). The internal morphology indicates that a small hollow, or pool, resided at the top of the stalagmite at the drip locus for much of the growth period. Speleothem growth hiatuses are indicated in the upper sections by changes in crystallography, morphology and colour of speleothem calcite and a thin red sediment layer (arrows in Fig. 2). Sub-samples (230–415 mg) were drilled from the polished surface for age determination by MC-ICPMS U–Th analysis to constrain the duration of non-depositional intervals. Several days after cutting and exposure to air, a white substance appeared on major discontinuities (marked by arrows in Fig. 2). In order to determine its mineralogical composition, X-ray diffraction method was employed.

### 3. Analytical methods

#### 3.1. U–Th procedures

Powdered samples were dissolved in  $\text{HNO}_3$  and spiked with a  $^{229}\text{Th}/^{236}\text{U}$  spike before being processed through ion exchange columns. Chemical procedures for separation of U and Th for MC-ICPMS, including dissolution, spiking and ion exchange separation, follow those described by Chen and Wasserburg (1981), Chen et al. (1986) and Luo et al. (1997). Instrumental protocols are reported in full in Hoffmann et al. (2007). In brief, U-series isotope measurements were undertaken using a ThermoFinnigan Neptune MC-ICPMS located

at the Bristol Isotope Group facilities, University of Bristol. The sample introduction system consists of a Cetac Aridus nebulizer equipped with a PFA spray chamber and a heated desolvating membrane. A nebulizer tip with a nominal uptake rate of  $50 \mu\text{l min}^{-1}$  was used for sample introduction. U and Th fractions are routinely measured separately in a 0.6 N HCl solution. A standard–sample bracketing procedure is adopted to derive correction factors for mass fractionation and Faraday cup to SEM gain (yield). For U measurements we use NBL-112a as bracketing U-standard. Thorium measurements are bracketed with an in-house  $^{229}\text{Th}$ – $^{230}\text{Th}$ – $^{232}\text{Th}$  Th-standard (TEDDi). Between sample and standard measurements, a wash procedure is undertaken and background intensities are recorded for correction of subsequent measurements. Darknoise of the SEM and baseline and gain calibration of the Faraday cups is done prior to a measurement sequence for online corrections. Deadtime and nonlinearity of the counting system are characterized and corrected for as described in Hoffmann et al. (2005). Ages corrected for an initial detrital component use a typical value for initial  $(^{232}\text{Th}/^{238}\text{U})_{\text{A0}}$  of  $1.34 \pm 0.54$ , based on bulk earth values and the assumption of secular equilibrium of daughter products. An attempt to refine this value using limited isochron methodology for sub-samples of the same age (K-18-C14L, R and M) did not yield significantly different values for the initial detrital component.

#### 3.2. Mineralogy

Qualitative mineralogical composition of material from the discontinuities was determined by X-ray diffraction methods (XRD). Measurements were done by PANalytical X'pert Pro theta–theta diffractometer equipped with a multilayer parabolic monochromator using  $\text{CuK}\alpha$  radiation, located in the Faculty of Natural Science, University of Zagreb. Material from the discontinuities was analysed directly on the speleothems, then scratched from the surface and, finally drilled out. Carbonate parts were also analysed in situ and drilled out from above and below hiatuses (Fig. 2).

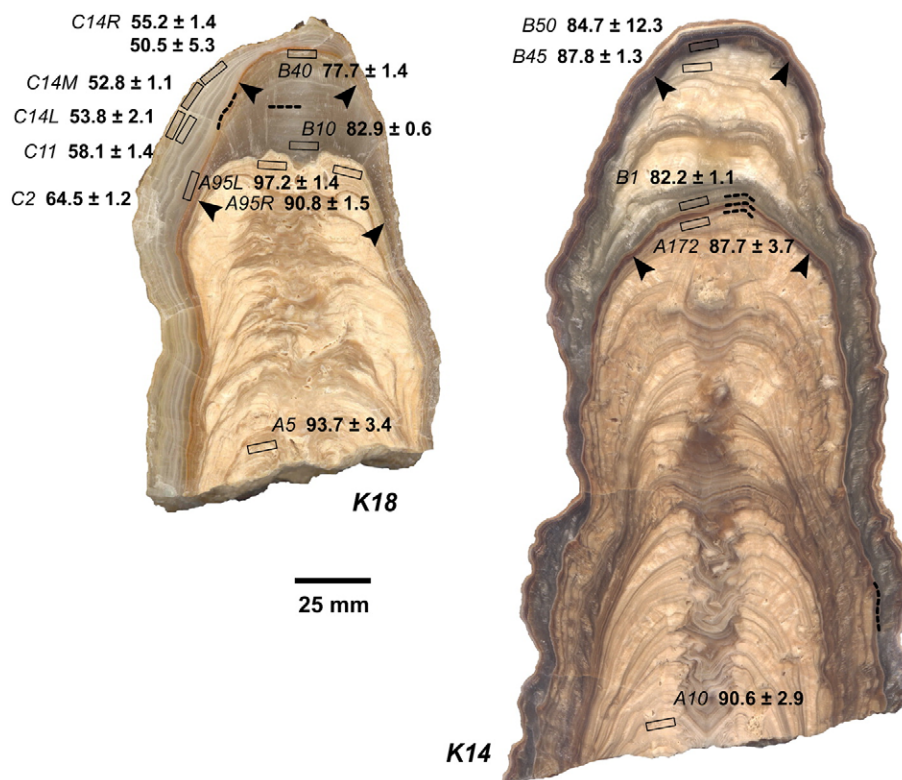


Fig. 2. Longitudinal sections of the speleothems K-14 and K-18 with U–Th ages ( $\pm 2\sigma$  uncertainty) and sub-sample locations. Also shown with black dashed lines are sub-sample locations of XRD analyses. White precipitate appeared along discontinuities marked by arrows after sectioning. (Scale bar 25 mm).

#### 4. Results and discussion

Uranium concentrations of measured sub-samples are low (30–70 ng g<sup>-1</sup>) and errors are typically 1 to 6% (2σ) (Table 1), depending on the extent of detrital contamination. The U–Th age range of sub-samples is ~93 to 54 ka. Most sub-samples have yielded ages in correct stratigraphic order. There are two anomalous results for material that may have been subject to post-depositional alteration during periods of submergence: K-18-A95L has a significantly older value than its stratigraphically equivalent sub-sample, A95R, with (<sup>234</sup>U/<sup>238</sup>U)<sub>A0</sub> closer to that of ocean water (present value for Mediterranean water = 1.149, Delanghe et al., 2002) (Fig. 3), suggesting a possible marine influence. Calcite sampled for A95L may have been more susceptible to post-depositional alteration because it is more porous than A95R, which was sampled from a region of denser, banded calcite. A similar situation occurs with K-14-B45, which is much older than the sub-sample below, K-14-B1. Again, this material is less dense than the sub-sample immediately above, K-14-B40. Combining the stratigraphically consistent data for both samples, it appears that three phases of growth are observed: K-18 grew from >93 ka to ~90 ka, ~82 ka to ~77 ka and from ~64 ka to ~54 ka, and, stalagmite K-14 from >90 ka to ~87 ka and for a short period ~82 ka.

According to the age–axial length relationship, the deposition of stalagmites K-14 and K-18 prior to the first submergence during MIS 5a was fast with growth rates of 5.3 and 3.0 cm/ka, respectively. It indicates favourable conditions with appropriate humidity and vegetation cover that resulted in precipitation of porous and inhomogeneous calcite. After the first transgression, precipitation of K-14 continued in the same fast-growing manner, whereas K-18 recorded a lower deposition rate (0.6 cm/ka) of well bedded and compact calcite during less favourable (colder) MIS 4 period.

In situ XRD measurements in the region marked by red layer and precipitation of white substance after sectioning and cutting of both speleothems indicated that halite and gypsum were precipitated in addition to calcite. No evidence for gypsum was observed in scratched and drilled sub-samples of spelean calcite, as well as for in situ analyses of the speleothem growth just above and below the hiatuses, where only small peaks for halite were found in addition to calcite. Minerals recorded along hiatuses (calcite, gypsum and halite) are

common cave minerals, but this assemblage also coincides with the suite of minerals that precipitate due to the evaporation of seawater (Ca-carbonates, gypsum, anhydrite, halite and K–Mg chlorides, arranged from less to the most soluble, Seibold and Berger, 1996). Halite could, presumably, crystallize from the seawater that penetrated through the porous parts of speleothems due to its high concentration in the seawater, but it is unlikely that gypsum precipitated from the same waters. It is more likely that it has been precipitated in situ at a time of exposure to marine conditions during sea-level regression.

We consider the hiatuses in these stalagmites to represent significant changes in environmental conditions in addition to submergence during high sea stands. Along with changes in the morphology, crystallography and colour of calcite, initial <sup>234</sup>U/<sup>238</sup>U also shows abrupt shifts between growth phases (Fig. 3) indicating substantial differences between the hydrological regimes for each phase of growth. In accordance with obtained U–Th ages, we can assume that deposition of speleothems K-18 had been more or less continuous in subaerial conditions from >93 to ~90 ka, from ~82 to ~77 ka and from ~64 to 54 ka, whereas K-14 had been precipitating from >90 to ~87 ka and for a brief period at 82 ka. Hiatuses recorded in periods 90–82 ka and 77–64 ka in K-18 and 87–82 ka in K-14, probably relate to sea-level oscillation which can be attributed to MIS 5a interstadial that was marked with two distinct sea-level highstands (double peak) at ~84 and ~77 ka which has also been recognised from coralline deposits on the uplifted island of Barbados (Potter and Lambeck, 2004; Potter et al., 2004; Schellmann and Radtke, 2004a,b; Schellmann et al., 2004; Radtke and Schellmann, 2005). According to our results, these sea-level highstands should have been higher than –14 m and lowstand was below –18 m (Fig. 4). Submergence of speleothem K-18 (–18.8 m) at ~90 ka ago and K-14 (–14.5 m) at ~87 ka ago could suggest a rapid sea-level rise with a rate of 1.4 m/ka, followed also by an abrupt sea-level fall. While it is possible that hiatuses can be formed by submergence in small pools perched above the local water table (or sea level), we consider this very unlikely in such a mature coastal karst terrain.

Comparing our results to the ice-volume equivalent global sea-level curve (Lambeck and Chappell, 2001), a difference of at least ~13–17 m is evident (Fig. 4) which would require an uplift at a rate of 0.15–

**Table 1**  
U and Th concentrations, isotope ratios and U–Th ages of speleothems from U Vode Pit (Krk Island).

Sample	Sub-sample	Distance along growth axis (mm)	Sample ID	<sup>238</sup> U (ng g <sup>-1</sup> )	<sup>232</sup> Th (ng g <sup>-1</sup> )	Measured			Age (ka)		<sup>234</sup> U/ <sup>238</sup> U <sub>A0</sub> (Corrected)
						( <sup>230</sup> Th/ <sup>232</sup> Th) <sub>A</sub>	( <sup>230</sup> Th/ <sup>238</sup> U) <sub>A</sub>	( <sup>234</sup> U/ <sup>238</sup> U) <sub>A</sub>	(Uncorrected)	(Corrected)	
K-18	C14L	157	BIG-UTH-F-05	33.4 ± 0.1	3.25 ± 0.01	17.2 ± 0.5	0.551 ± 0.015	1.352 ± 0.007	55.7 ± 2.0	53.8 ± 2.1	1.419 ± 0.009
K-18	C14R	157	BIG-UTH-F-06	38.8 ± 0.2	4.00 ± 0.01	17.1 ± 0.3	0.575 ± 0.009	1.382 ± 0.007	57.1 ± 1.2	55.2 ± 1.4	1.458 ± 0.009
K-18	C14R	157	BIG-UTH-F-06	34.4 ± 0.1	3.46 ± 0.01	17.6 ± 1.6	0.581 ± 0.046	1.492 ± 0.006	52.2 ± 5.2	50.5 ± 5.3	1.582 ± 0.012
K-18	C14M	157	BIG-UTH-F-17	34.8 ± 0.2	3.16 ± 0.01	18.5 ± 1.0	0.548 ± 0.007	1.369 ± 0.004	54.5 ± 0.9	52.8 ± 1.1	1.438 ± 0.006
K-18	C11	154	BIG-UTH-F-04	35.8 ± 0.3	1.05 ± 0.01	61.3 ± 1.7	0.591 ± 0.010	1.391 ± 0.007	58.6 ± 1.4	58.1 ± 1.4	1.464 ± 0.008
K-18	C2	144	BIG-UTH-F-03	66.5 ± 0.5	2.03 ± 0.01	59.3 ± 1.3	0.593 ± 0.008	1.295 ± 0.005	65.1 ± 1.2	64.5 ± 1.2	1.357 ± 0.005
K-18	B40	140	BIG-UTH-F-02	65.4 ± 0.3	0.94 ± 0.01	138.6 ± 2.7	0.649 ± 0.008	1.246 ± 0.005	78.0 ± 1.4	77.7 ± 1.4	1.308 ± 0.005
K-18	B10	115	BIG-UTH-A-259	48.7 ± 0.1	1.03 ± 0.00	96.9 ± 0.5	0.669 ± 0.003	1.229 ± 0.005	83.3 ± 0.6	82.9 ± 0.6	1.291 ± 0.003
K-18	A95L	99	BIG-UTH-A-260	90.2 ± 0.3	10.69 ± 0.03	17.6 ± 0.1	0.683 ± 0.002	1.124 ± 0.002	99.9 ± 0.7	97.2 ± 1.4	1.167 ± 0.004
K-18	A95R	99	BIG-UTH-A-261	80.6 ± 0.3	10.79 ± 0.03	15.3 ± 0.1	0.669 ± 0.003	1.143 ± 0.003	93.9 ± 0.7	90.8 ± 1.5	1.191 ± 0.005
K-18	A5	14	BIG-UTH-F-01	52.1 ± 0.2	4.38 ± 0.05	24.7 ± 0.6	0.679 ± 0.015	1.146 ± 0.005	95.6 ± 3.3	93.7 ± 3.4	1.194 ± 0.006
K-14	B50	232	BIG-UTH-A-236	60.9 ± 0.1	5.71 ± 0.2	2.3 ± 0.04	0.718 ± 0.011	1.122 ± 0.003	108.8 ± 2.8	84.7 ± 12.3	1.193 ± 0.031
K-14	B45	224	BIG-UTH-A-258	67.1 ± 0.2	7.16 ± 0.02	18.4 ± 0.1	0.642 ± 0.002	1.125 ± 0.003	90.3 ± 0.6	87.8 ± 1.3	1.165 ± 0.004
K-14	B1	182	BIG-UTH-A-235	44.9 ± 0.1	1.39 ± 0.01	62.2 ± 0.5	0.630 ± 0.005	1.166 ± 0.003	82.9 ± 1.0	82.2 ± 1.1	1.202 ± 0.003
K-14	A172	175	BIG-UTH-A-234	69.6 ± 0.1	15.53 ± 0.06	8.6 ± 0.1	0.631 ± 0.011	1.089 ± 0.003	93.1 ± 2.5	87.7 ± 3.7	1.115 ± 0.005
K-14	A10	0	BIG-UTH-F-25	100.3 ± 0.7	21.1 ± 0.4	9.3 ± 0.2	0.638 ± 0.008	1.082 ± 0.002	95.8 ± 2.0	90.6 ± 2.9	1.112 ± 0.004

Analytical errors are 2σ.

$(^{230}\text{Th}/^{238}\text{U})_A = 1 - e^{-\lambda_{230}T} + [(^{234}\text{U}/^{238}\text{U})_A - 1] \cdot [\lambda_{230}/(\lambda_{230} - \lambda_{234})](1 - e^{-(\lambda_{230} - \lambda_{234})T})$ , where  $T$  is the age.

Decay constants are  $9.1577 \times 10^{-6} \text{ yr}^{-1}$  for <sup>230</sup>Th,  $2.8263 \times 10^{-6} \text{ yr}^{-1}$  for <sup>234</sup>U (Cheng et al., 2000).

The degree of detrital <sup>230</sup>Th contamination is indicated by the measured (<sup>230</sup>Th/<sup>232</sup>Th)<sub>A</sub> activity ratio and age corrections were calculated using an average crustal (<sup>232</sup>Th/<sup>238</sup>U) value of  $1.34 \pm 0.67$ .

0.25 mm/a. However, a significant discrepancy of MIS 5a highstand records is noted worldwide, from both tectonically stable (Bahamas, Bermuda, Cayman Islands etc.) and tectonically unstable regions (Barbados, New Guinea and Huon Peninsula). Recorded MIS 5a highstand positions, relative to the present sea level, range from  $-30$  m to  $+10$  m (see Coyne et al., 2007; therein references and Fig. 18). In the European region, records from phreatic overgrowths on submerged speleothems from S and SE coasts of Mallorca also show aberration from the predicted global MIS 5a sea-level stand ( $\sim 1.5$  m above the present) (Onac et al., 2006).

According to the glacio-hydro-isostatic model for the last glacial-interglacial cycle, the Adriatic basin is generally subsiding (Lambeck and Purcell, 2005). Also, recent studies on late Holocene notches and submerged archaeological remnants along the Northern Adriatic coast reconstructed the subsiding history of this area, enhanced by coseismic tectonics. Nevertheless, proposed uplift from the last 80 ka should not be in contradiction with the recent subsidence because the studied area is situated between the eastern converging boundary of Adria plate (along the axis of the Dinaric Alps) to the northeast and an active tectonic boundary, dividing Adria plate into NW and SE tectonic blocks, to the southwest (Oldow et al., 2002). Such a position can support the possibility of long term regional uplift and episodic tectonic subsidence, which is common in convergence zones (Ferranti et al., 2007). Recent GPS geodetic measurements recorded an

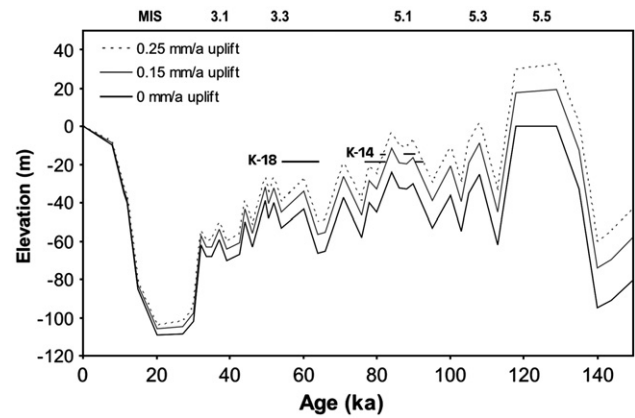


Fig. 4. Submerged speleothems K-14 and K-18 plotted against the global sea-level curve (Lambeck and Chappell, 2001) and relative sea-level curves according to the proposed uplift of 0.15–0.25 mm/a. MIS – marine isotope stage.

uplift of more than 10 mm/a of SE part of Krk Island relative to the Graz station, and horizontal velocity of 10 mm/a towards NE (Altiner et al., 2006), however, these data should be taken with caution and may apply exclusively to most recent times, because the aforementioned archaeological submerged remnants (Fouache et al., 2000; Antonioli et al., 2007) do not support such a rapid uplift.

## 5. Conclusion

We have dated two submerged stalagmites from the Eastern Adriatic coast to constrain the timing of sea-level events marked by two distinctive hiatuses in deposition. The growth hiatuses presented here are foremost chronological markers. They do not provide sea-level indicators in the strictest sense and cannot be utilised to solve what is known as the '80 ka' problem (Wehmiller et al., 2004), i.e. the wide range of current estimates from disparate location on the globe. They do offer constraints on temporal uplift if other model evidence is assumed, however. Hiatuses were characterized by changes in morphology, crystallography and colour and bordering reddish layer. A mineral assemblage of calcite, gypsum and halite appeared along the discontinuities on sectioning and exposure to air, and this is indicative of previous evaporation of seawater and hence marine conditions. Based on obtained U–Th ages and mineralogical composition, sea-level changes could be reconstructed as follows (assuming no tectonic adjustment):

- (i) precipitation of subaerial calcite in K-18 indicates that relative sea level was lower than  $-18.8$  m from  $>93$  to  $\sim 90$  ka, from  $\sim 82$  to  $\sim 77$  ka and from  $\sim 64$  to  $\sim 54$  ka. Growth periods in K-14 at  $-14.5$  m indicate that the sea level was lower than  $-14.5$  m from  $>90$  to  $\sim 87$  ka and for a short period at  $\sim 82$  ka.
- (ii) Speleothem growth hiatuses with fine red clays and marine salts indicate that relative sea level was likely to be higher than  $-18.8$  m from  $\sim 90$  ka to  $\sim 82$  ka and from  $\sim 77$  ka to  $\sim 64$  ka, and higher than  $-14.5$  m between  $\sim 87$  and  $\sim 82$  ka.

The periods of non-deposition probably caused by marine transgression coincide with high sea-level double peak at  $\sim 84$  and  $\sim 77$  ka BP within MIS 5a recorded in Barbados (Potter and Lambeck, 2004; Potter et al., 2004; Schellmann and Radtke, 2004a,b; Schellmann et al., 2004; Radtke and Schellmann, 2005). Present speleothem depths of  $-14.5$  m and  $-18.8$  m with recorded periods of marine conditions would indicate MIS 5a high sea-level stands of at least  $-14$  m in case of stable conditions, but it is more likely that there was a long term regional tectonic uplift of 0.15–0.25 mm/a with episodic subsidence events generated by collision of Adria microplate with European continent.

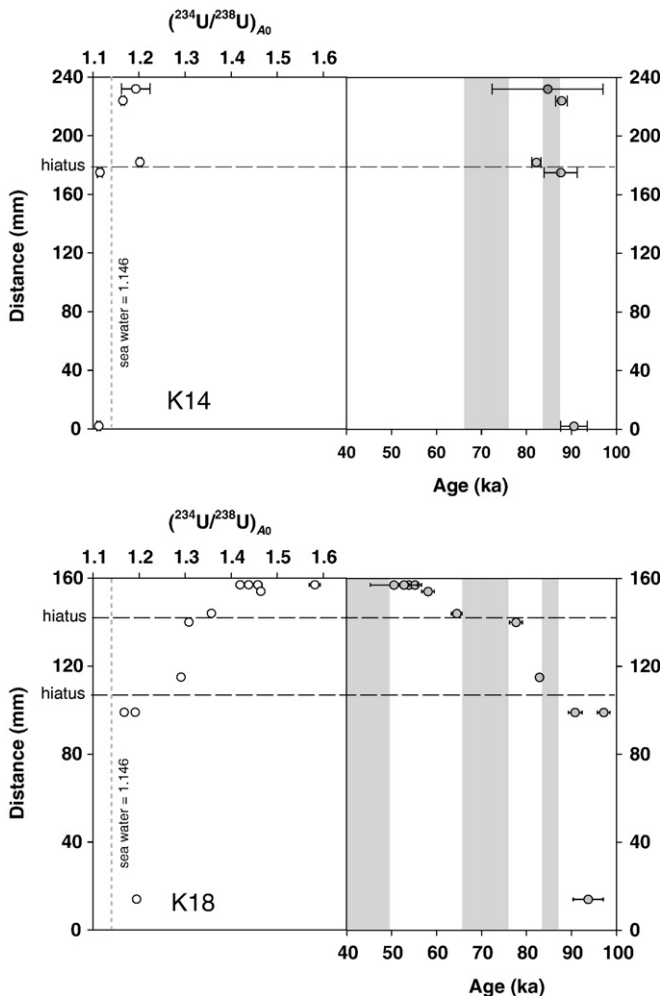


Fig. 3. Age and  $(^{234}\text{U}/^{238}\text{U})_{A0}$  along growth axis for speleothems K-14 and K-18. Growth hiatuses marked with horizontal dashed line, open seawater  $(^{234}\text{U}/^{238}\text{U})_{A0}$  with vertical dashed line. Maximum period of submergence based on both samples indicated by vertical shaded area (timing of final submergence most likely to be during last deglacial period after 10 ka).

## Acknowledgements

We would like to thank Coimbra Group association who enabled M. Surić, through its Hospitality Scheme, to undertake research at the School of Geographical Sciences, University of Bristol. We also thank speleodivers B. Jalžić, from Croatian Natural History Museum, and V. Jalžić, from the Institute for the Palaeontology and Geology of the Quaternary Period (Croatian Academy of Sciences and Arts) for providing samples from the submerged pit.

## References

- Altiner, Y., Marjanović, M., Medved, M., Rasić, L.J., 2006. Active deformation of the Northern Adriatic region: result from the CRODYN geodynamical experiment. In: Pinter, N., et al. (Ed.), *The Adria Microplate: GPS Geodesy, Tectonics and Hazards*. Springer, Dordrecht, pp. 257–268.
- Antonoli, F., Bard, E., Potter, E.K., Silenzi, S., Improta, S., 2004. 215-ka history of sea-level oscillations from marine and continental layers in Argentarola Cave speleothems (Italy). *Glob. Planet. Change* 43 (1–2), 57–78.
- Antonoli, F., Antidei, M., Lambeck, K., Auriemma, R., Gaddi, D., Furlani, S., Orrù, P., Solinas, E., Gaspari, A., Karinja, S., Kovačić, V., Surace, L., 2007. Sea-level change during the Holocene in Sardinia and in the northeastern Adriatic (central Mediterranean Sea) from archaeological and geomorphological data. *Quat. Sci. Rev.* 26, 2463–2486.
- Bard, E., Antonoli, F., Silenzi, S., 2002. Sea-level during the penultimate interglacial period based on a submerged stalagmite from Argentarola Cave (Italy). *Earth Planet. Sci. Lett.* 196 (3–4), 135–146.
- Benac, Č., Juračić, M., Bakran-Petricoli, T., 2004. Submerged tidal notches in the Rijeka Bay NE Adriatic Sea: indicators of relative sea-level change and of recent tectonic movements. *Mar. Geol.* 212, 21–33.
- Benac, Č., Juračić, M., Blašković, I., 2008. Tidal notches in Vinodol Channel and Bakar Bay, NE Adriatic Sea: indicators of recent tectonics. *Mar. Geol.* 248 (3–4), 151–160.
- Blašković, I., 1999. Tectonics of part of the Vinodol Valley within the model of the continental crust subduction. *Geol. Croat.* 52 (2), 153–189.
- Cattaneo, A., Correggiari, A., Langone, L., Trincardi, F., 2003. The late-Holocene Gargano subaqueous delta, Adriatic shelf: sediment pathways and supply fluctuations. *Mar. Geol.* 193, 61–91.
- Chappell, J., Shackleton, N.J., 1986. Oxygen isotopes and sea level. *Nature* 324, 137–140.
- Chen, J.H., Wasserburg, G.J., 1981. Isotopic determination of uranium in picomole and subpicomole quantities. *Anal. Chem.* 53 (13), 2060–2067.
- Chen, J.H., Edwards, R.L., Wasserburg, G.J., 1986. U-238, U-234, Th-232 in seawater. *Earth Planet. Sci. Lett.* 80, 241–251.
- Cheng, H., Edwards, R.L., Hoff, J.A., Gallup, C.D., Richards, D.A., Asmerom, Y., 2000. Determination of the half-lives of  $^{234}\text{U}$  and  $^{230}\text{Th}$ . *Chem. Geol.* 169, 17–33.
- Correggiari, A., Roveri, M., Trincardi, F., 1996. Late Pleistocene and Holocene evolution of the North Adriatic Sea. *Quaternario* 9 (2), 697–704.
- Coyne, M.K., Jones, B., Ford, D., 2007. Highstands during Marine Isotope Stage 5: evidence from the Ironshore Formation of Grand Cayman, British West Indies. *Quat. Sci. Rev.* 26 (3–4), 536–559.
- Cutler, K.B., Edwards, R.L., Taylor, F.W., Cheng, H., Adkins, J., Gallup, C.D., Cutler, P.M., Burr, G.S., Bloom, A.L., 2003. Rapid sea-level fall and deep-ocean temperature change since the last interglacial period. *Earth Planet. Sci. Lett.* 206 (3–4), 253–271.
- Delanghe, D., Bard, E., Hamelin, B., 2002. New TIMS constraints on the uranium-238 and uranium-234 in seawaters from the main ocean basins and the Mediterranean Sea. *Mar. Chem.* 80 (1), 79–93.
- Dutton, A., Scicchitano, G., Monaco, C., Desmarchelier, J.M., Antonoli, F., Lambeck, K., Esat, T.M., Fifield, L.K., McCulloch, M.T., Mortimer, G., 2009. Uplift rates defined by U-series and  $^{14}\text{C}$  ages of serpulid-encrusted speleothems from submerged caves near Siracusa, Sicily (Italy). *Quat. Geochronol.* 4, 2–10.
- Faivre, S., Fouache, E., 2003. Some tectonics influences on the Croatian shoreline evolution in the last 2000 years. *Z. Geomorphol. N. F.* 47 (4), 521–537.
- Ferranti, L., Monaco, C., Antonoli, F., Maschio, L., Kershaw, S., Verrubbi, V., 2007. The contribution of regional uplift and coseismic slip to the vertical crustal motion in the Messina Straits, southern Italy: evidence from raised Late Holocene shorelines. *J. Geophys. Res.* 112, B06401.
- Fornós, J.J., Gelabert, B., Ginés, A., Ginés, J., Tuccimei, P., Vesica, P., 2002. Phreatic overgrowths on speleothems: a useful tool in structural geology in littoral karstic landscapes. The example of eastern Mallorca (Balearic Islands). *Geodin. Acta* 15, 113–125.
- Fouache, E., Faivre, S., Dufaure, J.-J., Kovačić, V., Tassaux, F., 2000. New observation on the evolution of the Croatian shoreline between Poreč and Zadar over the past 2000 years. *Z. Geomorphol.* 122, 33–46.
- Garašić, M., 2006. Found and documented deepest speleothems in the sea (in Croatian). *Speleolog. Croat.* 7, 58.
- Hearty, P.J., Miller, G.H., Stearns, C.E., Szabo, B.J., 1986. Aminostratigraphy of Quaternary shorelines in the Mediterranean basin. *Geol. Soc. Amer. Bull.* 97, 850–858.
- Hoffmann, D.L., Richards, D.A., Elliott, T.R., Smart, P.L., Coath, C.D., Hawkesworth, C.J., 2005. Characterisation of secondary electron multiplier nonlinearity using MC-ICPMS. *Int. J. Mass Spectrom.* 244 (2–3), 97–108.
- Hoffmann, D.L., Prytulak, J., Richards, D.A., Elliott, T., Coath, C.D., Smart, P.L., Scholz, D., 2007. Procedures for accurate U and Th isotope measurements by high precision MC-ICPMS. *Int. J. Mass Spectrom.* 264 (2–3), 97–109.
- Lambeck, K., 1995. Late Pleistocene and Holocene sea-level change in Greece and south-western Turkey: a separation of eustatic, isostatic, and tectonic contributions. *Geophys. J. Int.* 122, 1022–1044.
- Lambeck, K., Bard, E., 2000. Sea level changes along the French Mediterranean coast from the past 30,000 years. *Earth Planet. Sci. Lett.* 175, 203–222.
- Lambeck, K., Chappell, J., 2001. Sea level change through the last glacial cycle. *Science* 292, 679–686.
- Lambeck, K., Purcell, A., 2005. Sea-level change in Mediterranean Sea since the LGM: model predictions for tectonically stable areas. *Quat. Sci. Rev.* 24, 1969–1988.
- Lea, D.W., Martin, P.A., Pak, D.K., Spero, H.J., 2002. Reconstructing a 350 ky history of sea level using planktonic Mg/Ca and oxygen isotope records from a Cocos Ridge core. *Quat. Sci. Rev.* 21, 283–293.
- Lundberg, J., Ford, D.C., 1994. Late Pleistocene sea level change in the Bahamas from mass spectrometric U-series dating of submerged speleothem. *Quat. Sci. Rev.* 13 (1), 1–14.
- Luo, X., Rehkämper, M., Lee, D.C., Halliday, A.N., 1997. High precision  $^{230}\text{Th}/^{232}\text{Th}$  and  $^{234}\text{U}/^{238}\text{U}$  measurements using energy-filtered ICP magnetic sector multiple collector mass spectrometry. *Int. J. Mass Spectrom.* 171 (1–3), 105–117.
- Muhs, D.R., Kennedy, G.L., Rockwell, T.K., 1994. Uranium-series ages of marine terrace corals from the Pacific coast of North America and implications for last-interglacial sea level history. *Quat. Res.* 42, 72–87.
- Murray-Wallace, C.V., 2002. Pleistocene coastal stratigraphy, sea-level highstands and neotectonism of the southern Australian passive continental margin—a review. *J. Quat. Sci.* 17, 469–489.
- Oldow, J.S., Ferranti, L., Lewis, D.S., Campbell, J.K., D’Argenio, B., Catalano, R., Pappone, G., Carmignani, L., Conti, P., Aiken, C.L.V., 2002. Active fragmentation of Adria, the north African promontory, central Mediterranean orogen. *Geology* 30 (9), 779–782.
- Onac, B., Fornós, J.J., Ginés, J., Ginés, A., Tuccimei, P., Peate, D.W., Björck, S., 2006. Sea-level position at ~80 ka based on phreatic overgrowths on speleothems from Mallorca. In: Onac, B., Tămaş, T., Constantin, S., Perşoiu, A. (Eds.), *Archives of Climate Change in Karst*, Proceedings of the Symposium Climate Change: the Karst Record (IV), 26–29 May 2006, Băile Herculane, Romania, Karst Water Institute, pp. 189–191.
- Picha, F.J., 2002. Late orogenic strike-slip faulting and escape tectonics in frontal Dinarides–Hellenides, Croatia, Yugoslavia, Albania, and Greece. *Am. Assoc. Pet. Geol. Bull.* 86 (9), 1659–1671.
- Pirazzoli, P.A., 1996. *Sea Level Changes – the Last 20,000 Years*. Wiley & Sons, Chichester, 211 pp.
- Potter, E.K., Lambeck, K., 2004. Reconciliation of sea-level observations in the Western North Atlantic during the last glacial cycle. *Earth Planet. Sci. Lett.* 217 (1–2), 171–181.
- Potter, E.K., Esat, T.M., Schellmann, G., Radtke, U., Lambeck, K., McCulloch, M.T., 2004. Suborbital-period sea-level oscillations during marine isotope substages 5a and 5c. *Earth Planet. Sci. Lett.* 225, 191–204.
- Radtke, U., Schellmann, G., 2005. Timing and magnitude of sea level change during MIS 5 derived from Barbados coral reef terraces: a critical literature review and new data. *J. Coast. Res.* 42, 52–62.
- Richards, D.A., Dorale, J.A., 2003. Uranium-series chronology and environmental applications of speleothems. *Rev. Mineral. Geochem.* 52, 407–460.
- Richards, D.A., Smart, P.L., Edwards, R.L., 1994. Maximum sea levels for the last glacial period from U-series ages of submerged speleothems. *Nature* 367, 357–360.
- Schellmann, G., Radtke, U., 2004a. *The Marine Quaternary of Barbados*. Köln Geographische Schriften, vol. 81, 137 pp.
- Schellmann, G., Radtke, U., 2004b. A revised morpho- and chronostratigraphy of the Late and Middle Pleistocene coral reef terraces on Southern Barbados (West Indies). *Earth-Sci. Rev.* 64 (3–4), 157–187.
- Schellmann, G., Radtke, U., Potter, E.K., Esat, T.M., McCulloch, M.T., 2004. Comparison of ESR and TIMS U/Th dating of marine isotope stage (MIS) 5e, 5c, and 5a coral from Barbados – implications for palaeo sea-level changes in the Caribbean. *Quat. Int.* 120 (1), 41–50.
- Seibold, E., Berger, W.H., 1996. *The Sea Floor – an Introduction to Marine Geology*, third ed. Springer, Berlin, 356 pp.
- Siddall, M., Rohling, E.J., Almqvist-Labin, A., Hemleben, Ch., Meischner, D., Schmelzer, I., Smeed, D.A., 2003. Sea-level fluctuations during the last glacial cycle. *Nature* 423, 853–858.
- Surić, M., 2006. Late Pleistocene–Holocene palaeoenvironmental changes – records from submerged speleothems from the Eastern Adriatic Sea (Croatia) (in Croatian), PhD Thesis, Faculty of Natural Science, University of Zagreb, Croatia, 213 pp.
- Surić, M., Juračić, M., Horvatinčić, N., Krajar Bronić, I., 2005. Late Pleistocene–Holocene sea-level rise and the pattern of coastal karst inundation: records from submerged speleothems along the Eastern Adriatic Coast (Croatia). *Mar. Geol.* 214 (1–3), 163–175.
- Velić, I., 2007. Stratigraphy and palaeobiogeography of Mesozoic benthic foraminifera of the Karst Dinarides (SE Europe). *Geol. Croat.* 60 (1), 1–114.
- Vlahović, I., Tišljarić, J., Velić, I., Matičec, D., 2002. The Karst Dinarides are composed of relics of a single Mesozoic platform: facts and consequences. *Geol. Croat.* 55 (2), 171–183.
- Vlahović, I., Tišljarić, J., Velić, I., Matičec, D., 2005. Evolution of the Adriatic Carbonate Platform: palaeogeography, main events and depositional dynamics. *Palaeogeogr. Palaeoclimatol. Palaeoecol.* 220, 333–360.
- Vrhovec, T., Mihevc, A., Lauritzen, S.E., Lundberg, J., 2001. On the ages of the submerged stalactites from the pit near islet Galiola, Dalmatia, Croatia (in Slovenian). *Naše Jame* 43, 31–36.
- Waelbroeck, C., Labeyrie, L., Michel, E., Duplessy, J.C., McManus, J.F., Lambeck, K., Balbon, E., Labracherie, M., 2002. Sea-level and deep water temperature changes derived from benthic foraminifera isotopic records. *Quat. Sci. Rev.* 21, 295–305.
- Wehmler, J.F., Simmons, K.R., Cheng, H., Edwards, R.L., Martin-McNaughton, J., York, L.L., Krantz, D.E., Shen, C.C., 2004. Uranium-series coral ages from the US Atlantic coastal plain – the “80 ka problem” revisited. *Quat. Int.* 120, 3–14.